2023 IEEE/ASME International Conference on Advanced Intelligent Mechatronics (AIM)
June 28-30, 2023. Seattle, Washington, USA

An iterative method for solving the inverse kinematic problem of three-joints robotic fingers with distal coupling.

Jonatan Martín Escorcia-Hernández [1], Mathieu Grossard [1], Florian Gosselin [1], Clémence Dubois [1].

***Abstract*—This paper introduces a methodology for finding a solution to the inverse kinematic problem of underactuated manipulators composed of a three-link revolute joints planar mechanism with mechanical coupling. The proposed method consists in solving iteratively a set of algebraic equations defining the Inverse Kinematic Model (IKM) of a 3R mechanism whose rotational joints are first considered independent. The respect of the mathematical constraint due to the mechanical coupling between certains axes is taken into account in the procedure by introducing an internal variable whose value is updated iteratively. The value of this internal variable is increased at each iteration until the coupling relationship is satisfied. The proposed methodology is applied to solve the IKM of a multi-phalanx robotic finger whose kinematics follows a human-like finger coupling between the intermediate and distal phalanges.**

***Index Terms*—Inverse kinematics, Planar three-joints mechanisms, Robotic finger**

I. Introduction

Robotic systems can be classified according to their actuation architecture: fully-actuated (FA), if their number of actuators is equal to their number of joints, redundantly-actuated (RA) if their number of actuators is bigger than their number of joints, and under-actuated (UA) if their number of actuators is smaller to their number of joints [1]. These latter have certain advantages with respect to their FA and RA counterparts such as: reduced energy consumption, less number of mechanical elements, volume saving, and reduction of manufacturing costs [2]. The mentioned features have made UA systems a cornerstone for the design and subsequent manufacture of: legged robots [3], robotic arms [4], robotic wrists [5], underwater vehicles [6], and robotic hands [7] among others [8]. Some UA systems have been designed from a bio-inspired point of view such as legged manipulators and robotic hands, also known as multi-fingered grippers. Robotic hands incorporate a certain degree of anthropomorphism to carry out tasks performed by human hands, the under-actuation arising from the need to replicate the correlation of movement between the intermediate and distal phalanges of each finger. From a biological point of view there exist an interdependence between the distal interphalangeal (DIP) joint and the proximal interphalangeal (PIP) joint of the human fingers during the flexion/extension [9]. Such dependency results from biomechanical constraints produced by the actuation system of the fingers involving the flexor digitorum superfialis (FDS) and the flexor digitorum profundus (FDP) tendons used for the flexion of the finger and the extensor digitorum communist (EDC) tendon used for the extension [10]. Several robotic finger designs use mechanical couplings based on pulleys or gears to reproduce the dependence of movement between the PIP and DIP joints, resulting in UA systems. We can detail some examples of robotic hands whose fingers integrate a passive coupling between the DIP and the PIP joints, for instance: the DLR Hands [11], [12], which are formed by four fingers, each finger having four joints, among which only three are actuated (the joint that produces the abduction/adduction motion, and the joints of the proximal and intermediate phalanges used for flexion/extension), the distal phalanx being coupled to the intermediate one by using a pulley. The CEA dexterous hand [13] is another example. It is composed by five fingers, each one formed by a modular unit that includes three electric backdrivable motors used to pilot four joints used to regulate the abduction/adduction and flexion/extension motions. As in DLR hands, CEA dexterous hand makes use of a coupling mechanism to transfer the motion from the PIP joint to the DIP joint. Despite the fact that there are notable differences in the above examples in terms of actuation, transmission, and the number of fingers, all of them make use of three-links-planar mechanisms that attempt to emulate the three phalanges of a human finger. In the existing literature, it has been extensively documented the kinematic modeling (forward and inverse) of such three-links planar mechanisms considering the three joints as independently actuated [14], [15], [16]. In the case of the Forward Kinematic Model (FKM), the inclusion of a kinematic coupling does not considerably entail the way to find the FKM solution, and we can take advantage of classical formulations such as the Denavit-Hartenberg (D-H) notation. However, finding a solution to the Inverse Kinematic Model (IKM) becomes a very challenging procedure due to the kinematic restrictions imposed by the coupling. In the literature, it has been reported few methods to solve the IKM in underactuated 3R mechanisms with coupling. We can cite some relevant examples, for instance in [17], the problem is solved by using a multi-layered Artificial Neural-Network (ANN). The simulation results showed a good convergence between the desired positions in Cartesian space and the estimated ones. Nevertheless, the accuracy and the learning speed of the ANN depend on the appropriate tuning of four parameters of the learning algorithm. In [18], the IKM solution is an integral part of the process for generating optimal trajectories in Cartesian space for a prosthetic finger. The coupling constant between the PIP and DIP joints is

[1] J.M. Escorcia-Hernández, M. Grossard, F. Gosselin, and C. Dubois, are with Université Paris-Saclay, CEA, List, F-91120, Palaiseau, France. Emails: {jonatan.escorcia, mathieu.grossard, florian.gosselin, clemence.dubois, }@cea.fr

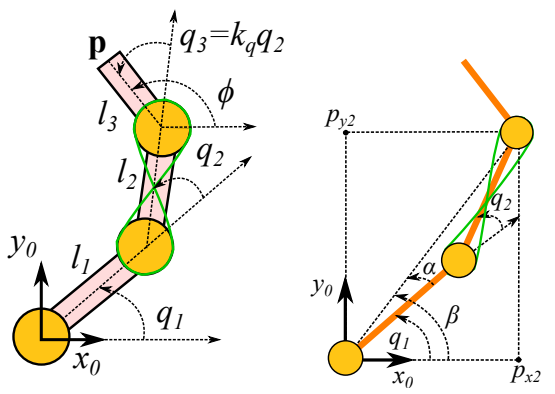

(a) Illustration of the main variables (b) Illustration of the auxiliary variables

Figure 1. Kinematic representation of the underactuated 3R mechanism with mechanical coupling.

computed by minimizing the maximum jerk in the finger joints. Then, the IKM is solved through a standard Newton-Raphson algorithm. Nevertheless, this method requires an appropriate initial guess value to converge to the local solution, and it may be computationally expensive.

In this paper, we propose a new methodology to solve the IKM for underactuated 3R mechanisms with kinematic coupling. The proposed method consists in solving iteratively the equations that define the IKM of this kind of mechanisms considering first the three revolute joints of the mechanism as "independently actuated" then introducing the coupling condition between the PIP and the DIP joints. The reminder of the paper is organized as follows: Section II describes in detail the problem of finding an IKM solution for underactuated 3R mechanisms with coupling between the PIP and DIP joints. The proposed solution used to address this problem is explained in Section III. In Section IV, we applied the proposed methodology to solve the IKM of a robotic finger that will be part of a future gripper dedicated to perform sterility testing processes. The validation of the proposed methodology in detailed in Section V, and finally, the conclusions of this study are discussed in Section VI.

II. Problem description

Let us consider the planar underactuated 3R mechanism with kinematic coupling depicted in Fig. 1, whose Cartesian space variables are denoted as $\mathbf{p} = [p_x \quad p_y]^T$, whereas the join space ones are represented as $\mathbf{q} = [q_1 \quad q_2 \quad q_3]^T$. The Forward Kinematic Model (FKM) establishes the Cartesian position of the manipulator given the joints' positions. In this case the equations describing the FKM are given as follows:

$$\begin{aligned} p_x &= l_1 \cos q_1 + l_2 \cos(q_1 + q_2) + l_3 \cos[q_1 + (1 + k_q)q_2] \\ p_y &= l_1 \sin q_1 + l_2 \sin(q_1 + q_2) + l_3 \sin[q_1 + (1 + k_q)q_2] \end{aligned} \tag{1}$$

where k_q is the coupling ratio. In order to compute the IKM, we should be able to solve the system of equations (1) by considering p_x and p_y as known parameters and, q_1, q_2 as unknown variables. Therefore, squaring the equations in (1), summing them and simplifying by means of trigonometric identities, leads to the following mathematical expression:

$$\begin{aligned} p_x^2 + p_y^2 - l_1^2 - l_2^2 - l_3^2 = 2l_1 l_2 \cos q_2 \\ +2l_1 l_3 \cos(q_2 + k_q q_2) + 2l_2 l_3 \cos k_q q_2 \end{aligned} \tag{2}$$

Equation (2) is a nonlinear equation with only one unknown q_2.

In the restrictive case of a coupling constant k_q as an integer number, existing methodologies based on Chebyshev polynomials are known [19]. In the more general case where k_q can take any real value (more likely in the practical case of mechanical coupling within poly-articulated mechanisms), this equation needs to be solved using a numerical approach, as it has no analytical solution.

III. Proposed solution

We introduce an auxiliary angle called ϕ, which represents the absolute orientation of the last link of the mechanism with respect to the abscissa axis (x_0 in this case, see Fig 1). If each joint is considered as independently actuated, then the angle ϕ should be considered as an input Cartesian space variable together with p_x and p_y. In the related literature, the orientation angle ϕ is crucial to obtain the IKM for 3R mechanism as detailed in [14], [15] and [16]. However, in this case, we have a system where the first and second joints are considered independently actuated, whereas the third joint is coupled to the second one. Although ϕ exists and its value can be computed in underactuated 3R with coupling, it cannot be considered as an input variable since its value is restricted to an unique value due to the coupling constant. The angle ϕ of the underactuated 3R mechanism with coupling is defined by the following equation:

$$\phi = q_1 + q_2 + q_3 = q_1 + (1 + k_q)q_2 \tag{3}$$

where q_3 is a variable that directly depends of the value of q_2, and the term $k_q q_2$ restricts ϕ to a unique orientation as a function of q_2. Therefore, we need to find the IKM solution that satisfy $q_3 = k_q q_2$. In order to find the IKM solution, we propose to solve iteratively the equations that define the IKM considering firstly all joints of the 3R mechanism as "independently actuated". As mentioned previously, when considering the system as fully actuated, it will be necessary to provide an initial value ϕ_{init} of ϕ for the any given value of p_x, p_y, and then start performing the calculations iteratively by slightly increasing the value of ϕ until the solution that satisfies the coupling condition is found. Thereby, the proposed method requires prior knowledge about the range of motion of the two actuated joints in order to define an appropriate initial value for ϕ. We can summarize the steps to compute IKM as illustrated in Figure 2.

Now, let us start with the formulation of the equations that allow finding the value of the joints as a function of the assigned position in the Cartesian space. Since p_x, p_y and ϕ_{init} are considered known, it is necessary to formulate an expression that takes into account only the subsystem constituted by the two first links. Therefore, the system of equations described in

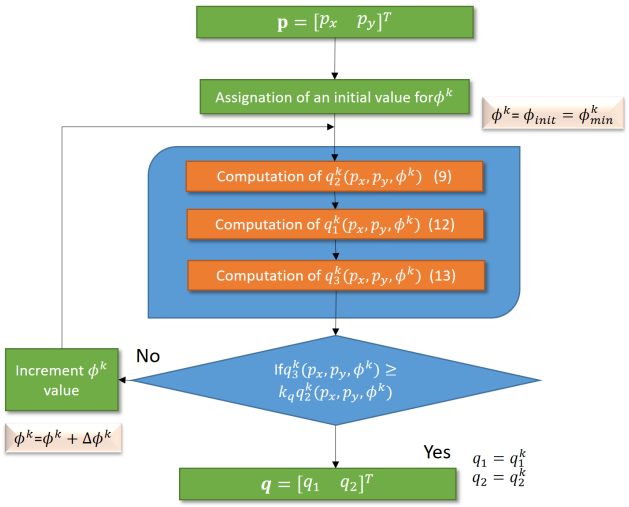

Figure 2. Workflow procedure for obtaining the IKM.

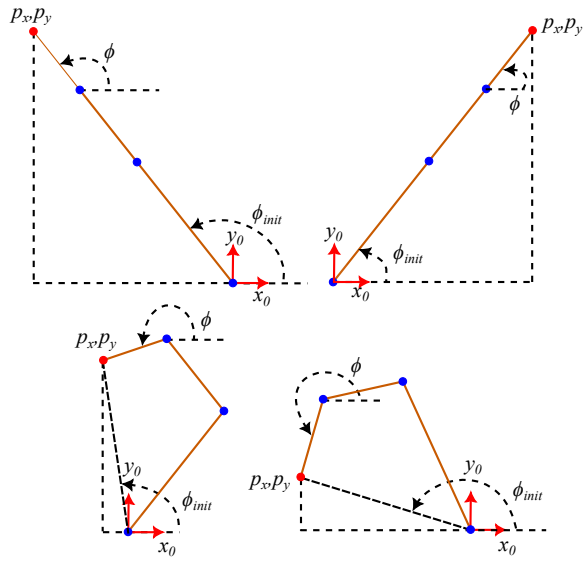

Figure 3. Illustration of several positions performed by a 3R mechanism where ϕ always satisfy $\phi \geq \phi_{init}$

(1) is reformulated by separating the known variables from the unknown ones, resulting in the following system of equations.

$$\begin{aligned} p_{x2}^k &= p_x - l_3 \cos\phi^k = l_1 \cos q_1 + l_2 \cos(q_1 + q_2) \\ p_{y2}^k &= p_y - l_3 \sin\phi^k = l_1 \sin q_1 + l_2 \sin(q_1 + q_2) \end{aligned} \tag{4}$$

where p_{x2}^k, and p_{y2}^k correspond to the position of the third joint of the manipulator measured from the origin frame as Fig. 1(b) illustrates, and the superscript k denotes the current value of the involved variable at the k^{th} iteration. By squaring and summing both equations of (4), the following expression is obtained:

$$\begin{aligned} (p_{x2}^k)^2 + (p_{y2}^k)^2 = l_1^2 + l_2^2 + 2l_1 l_2 [\cos q_1^k \cos(q_1^k + q_2^k) + \\ \sin q_1^k \sin(q_1^k + q_2^k)] \end{aligned} \tag{5}$$

By using trigonometric identities, the trigonometric functions in (5) can be simplified as:

$$\cos q_1^k \cos(q_1^k + q_2^k) + \sin q_1^k \sin(q_1^k + q_2^k) = \cos q_2^k \tag{6}$$

Therefore, (5) can be rewritten as:

$$\cos q_2^k = \frac{(p_{x2}^k)^2 + (p_{y2}^k)^2 - l_1^2 - l_2^2}{2 l_1 l_2} \tag{7}$$

A complementary sin function can be established as:

$$\sin q_2^k = \pm\sqrt{1 - \cos^2 q_2^k} \tag{8}$$

The term $\pm$ of (8), indicates that there are two pairs of possible solutions for q_1^k and q_2^k. In the case of q_2^k its value can be found as follows:

$$q_2^k = \arctan 2(\sin q_2^k, \cos q_2^k) \tag{9}$$

Once the value of q_2^k is found, we can proceed to calculate the angle q_1^k by using the auxiliary angles α^k and β^k as explained in [20]. The angle β^k is formulated by analyzing Fig 1(b).

$$\beta^k = \arctan 2(p_{2y}^k, p_{2x}^k) \tag{10}$$

The angle α^k can be formulated as follows:

$$\alpha^k = \arctan 2(l_2 \sin q_2^k, l_1 + l_2 \cos q_2^k) \tag{11}$$

Thereby, the angle q_1^k results from:

$$q_1^k = \beta^k - \alpha^k \tag{12}$$

Finally, the dependent joint q_3^k is computed by:

$$q_3^k = \phi^k - q_1^k - q_2^k \tag{13}$$

The equations (9), (12), and (13) are solved iteratively until satisfying the following condition:

$$q_3^k \geq k_q q_2^k \tag{14}$$

If the previous condition is satisfied, we can affirm that $q_1 = q_1^k$, and $q_2 = q_2^k$ yielding the solution of the IKM. It is worth to emphasize that this methodology is focused on finding the IKM of underactuated 3R mechanisms under the following constrains:

$$\begin{aligned} l_1 > l_2 > l_3 \\ q_2 \geq 0 \\ k_q \leq 1 \end{aligned} \tag{15}$$

Such constraints constitute key aspects in the kinematics of human-inspired robotic fingers. The first indicates that the proximal phalanx should be longer than the intermediate and distal phalanges, and the intermediate phalanx should be longer than the distal phalanx. The second constraint indicates that q_2, which is related to the PIP, cannot perform negative extension movements, which is the case for active movements of the index, middle, ring, and little fingers of the human hand [21]. Finally, the last constrain implies that the displacement of q_3 (DIP joint angle) will never be greater than that of q_2 (PIP joint angle), but it may be equal.

Regarding the selection of ϕ_{init}, since the true value ϕ is unknown when p_x and p_y are assigned, we have to choose ϕ_{init} relatively close and with a lower value than the unknown ϕ, because if we assign an initial value greater than the real one, the iteration process will fail to find a solution. If the mechanism satisfies the conditions established in (15), we can

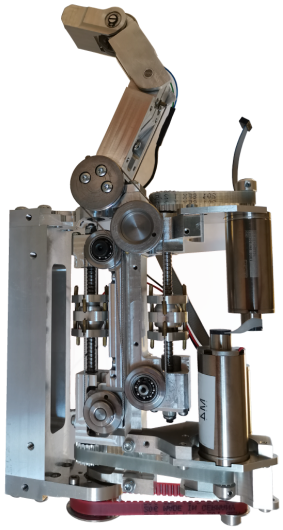

Figure 4. Modular finger unit prototype.

make use of the following formula to determine a suitable value for ϕ_{init}:

$$\phi_{init} = \arctan 2(p_y, p_x) \tag{16}$$

The previous expression guarantees that computed value for ϕ_{init} will be smaller and close to the unknown ϕ as is depicted in Figure 3.

Now, let us apply the described iterative method to compute the IKM of a modular robotic finger intended to be integrated into a future multi-fingered gripper whose phalanges design satisfies the constraints of (15).

IV. Case Study

The present case study shows the validation of our inverse kinematics algorithm using a modular robotic finger that will be integrated into a future multi-fingered gripper designed to perform sterility testing processes within the European project TraceBot [22]. The modular finger is composed of three phalanges (proximal, intermediate, and distal) connected to each other via three revolute joints used to perform flexion/extension motions. The finger incorporates an additional joint placed at the base to regulate its orientation. The finger makes use of three electric motors to drive remotely the four finger joints through a cable-based transmission yielding an underactuated 3-DoF configuration. Figure 4 illustrates the assembly of a robotic finger prototype, and Figure 5 depicts its kinematic configuration where the kinematic parameters are defined as follows: l_{1h}, and l_{1v} represent the horizontal and vertical offsets between the self-rotation joint and the proximal phalanx joint, and l_2, l_3, l_4 represent the lengths of the proximal, intermediate, and distal phalanges.

A. Inverse Kinematic modeling

The position variables of the 3-DoF TraceBot modular finger are denoted as follows: $\mathbf{p} = \begin{bmatrix} p_x & p_y & p_z \end{bmatrix}^T$ for the task space variables, and $\mathbf{q} = \begin{bmatrix} q_0 & q_1 & q_2 & q_3 \end{bmatrix}^T$ for the joint ones. It is worth to recall that q_3 is a dependent joint variable whose value is determined by the position of q_2. Unlike the general

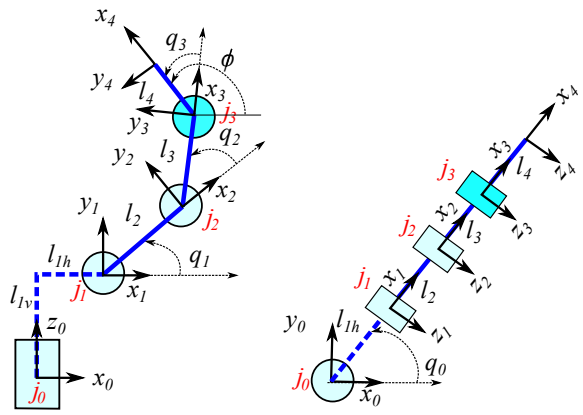

(a) Lateral view (b) Top view

Figure 5. Detailed illustration of the kinematic configuration of the 3-DoF TraceBot finger.

model of a 3R mechanism, in this case the finger has an additional joint at its basis for orientation purposes. Therefore, it is necessary to find its value before performing the iterative process used to find joint positioning of the finger phalanges. The self-rotation joint q_0, can be formulated by analyzing Figure 5(b) (with the hypothesis that $-60° \leq q_0 \leq 60°$):

$$q_0 = \begin{cases} \arctan 2\left(p_y, p_x\right), & p_x \geq 0 \\ \arctan 2\left(-p_x, p_y\right) - \pi/2, & p_x < 0 \end{cases} \tag{17}$$

The next step consists in performing the iterative computations in order to find the joint positions of the three phalanges of the finger that satisfy the kinematic coupling between the intermediate and distal phalanges. Following the procedure described in Section III, the position of the PIP joint (q_2), is determined by applying (9). However, the cosine function described in (7), must be reformulated as follows:

$$\cos q_2^k = \frac{\left(p_{x3}^k\right)^2 + \left(p_{y3}^k\right)^2 + \left(p_{z3}^k\right)^2 - l_2^2 - l_3^2}{2 l_2 l_3} \tag{18}$$

The auxiliary position variables p_{x3}^k, p_{y3}^k, and p_{z3}^k are formulated by clearing the Cartesian positioning equations, which are obtained by calculating the Forward kinematic model. For this case, the auxiliary position that separate the known data from the unknown data are:

$$\begin{aligned} p_{x3}^k =& p_x - (l_{1h} + l_4 \cos\phi^k)\cos q_0 = \\ & \cos q_0 [l_2 \cos q_1^k + l_2 \cos(q_1^k + q_2^k)] \\ p_{y3}^k =& p_y - (l_{1h} + l_4 \cos\phi^k)\sin q_0 = \\ & \sin q_0 [l_2 \cos q_1^k + l_3 \cos(q_1^k + q_2^k)] \\ p_{z3}^k =& p_z - l_{1v} - l_4 \sin\phi^k = l_2 \sin q_1^k + l_3 \sin(q_1^k + q_2^k) \end{aligned} \tag{19}$$

The angular displacement for the proximal phalanx (q_1) are determined by considering (12). However, the auxiliary angles α^k and β^k should be reformulated as follows:

$$\alpha^k = \arctan 2(l_3 \sin q_2^k, l_2 + l_3 \cos q_2^k) \tag{20}$$

$$\beta^k = \arctan 2(p_{z3}^k, s^k) \tag{21}$$

TABLE I
KINEMATIC PARAMETERS OF THE 3-DOF MODULAR FINGER.

Parameter	Description	Value
l_{1h}	Horizontal offset distance between j_0 and j_1	5 mm
l_{1v}	Vertical offset distance between j_0 and j_1	12.75 mm
l_2	Proximal phalanx length	62 mm
l_3	Intermediate phalanx length	37 mm
l_4	Distal phalanx length	28 mm
k_q	Coupling ratio	2/3

where the auxiliary term s^k is defined as:

$$s^k = \pm\sqrt{(p^k_{x3})^2 + (p^k_{y3})^2} \tag{22}$$

where the sign of s^k is chosen according to the following conditions, which involve the orientation of the finger q_0 in the xy-plane considering the aforementioned range of motion:

$$\text{sgn}(s^k) = \begin{cases} +, & p^k_{x3} > 0 \\ -, & p^k_{x3} \leq 0 \end{cases} \tag{23}$$

Finally, the position of the DIP joint is funded by implementing (13). And the iterative procedure ends when the coupling condition described in (14) is satisfied. The initial orientation angle considered for the iterative procedure ϕ_{init} described in (16) is reformulated for our case study considering the self-rotation angle q_0 as follows:

$$\phi_{init} = \arctan 2\left(p'_z, \pm\sqrt{p'^2_x + p'^2_y}\right) \tag{24}$$

where:

$$\begin{aligned} p'_x &= p_x - l_{1h}\cos q_0 \\ p'_y &= p_y - l_{1h}\sin q_0 \\ p'_z &= p_z - l_{1v} \end{aligned} \tag{25}$$

V. MODEL VALIDATION

This section presents the evaluation performed to validate the effectiveness of the proposed methodology for IKM calculation. For this section, we make use of the kinematic parameters of the finger described in Table 1. We select four desired points that lie within the workspace of the robotic finger. The workspace of the finger is bounded by the kinematic parameters and the following ranges of motion: $-60° \leq q_0 \leq 60°$, $45° \leq q_1 \leq 135°$, $0° \leq q_2 \leq 90°$, and $0° \leq q_3 \leq 60°$. The way to validate the IKM algorithm is based on simulation and real-time tests. In order to perform the numerical iterations, we define an increment constant value $\Delta\phi^k = 0.01$ rad. The obtained results are summarized in Table 2, in which the first column corresponds to the desired position in Cartesian space, the second one is the computed ϕ_{init}. The columns 3-6 of the table show the values obtained from the IKM solution, the seventh column denotes the resulting value for ϕ, the eighth column includes the number of required iterations used to find the IKM solution, the ninth column denotes the consumed time for all iterations, and the tenth column represents the absolute error of the approximation ε, which is computed as follows:

$$\varepsilon = ||FKM(q_0, q_1, q_2, q_3) - FKM(q_0, q_1, q_2, k_q q_2)||_2 \tag{26}$$

where FKM represents the forward kinematic model being evaluated with the values resulting form the IKM computations. The first FKM considers the value of q_3 resulting from the iterative process whereas the second one computes it by multiplying q_2 by the coupling constant. It is worth mentioning that each iteration is executed in $30\mu s$.

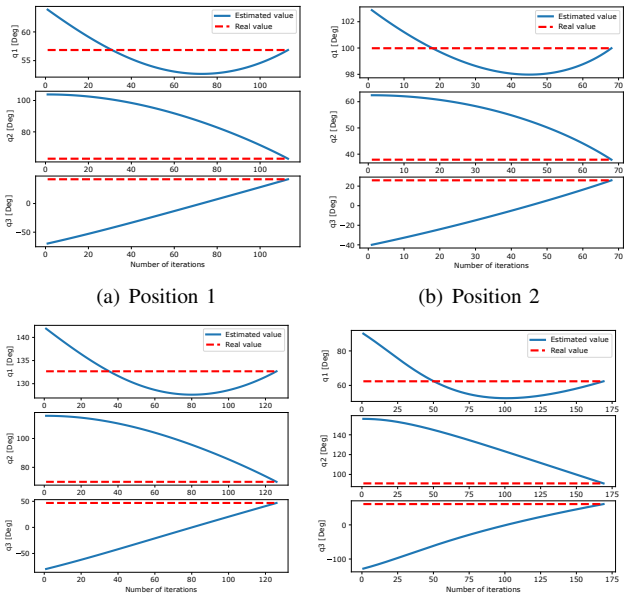

(a) Position 1 (b) Position 2

(c) Position 3 (d) Position 4

Figure 6. Evolution of the estimation of the joint space variables with respect to the number of iterations.

The resulting data of Table 2 is complemented with the information provided in Figure 6. This figure helps us to understand how the joint variables evolve during the computation process. By analyzing the obtained information, we can see that the number of iterations performed in the four desired points are relatively low, which is positive since the computation time is also relatively low. Therefore, the proposed solution is suitable

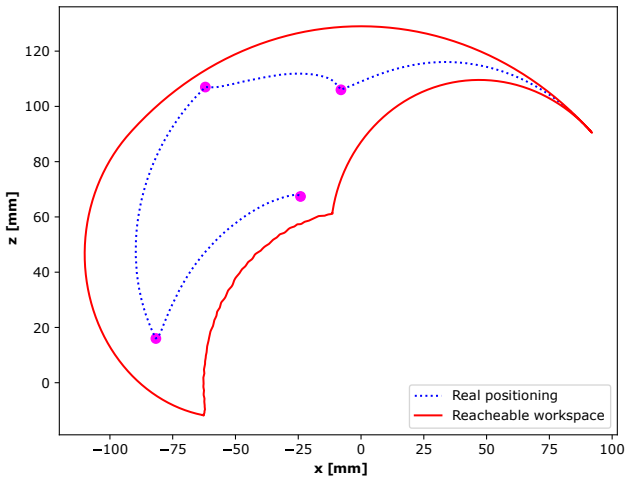

Figure 7. Positioning of the modular robotic finger in one plane by performing the IKM.

TABLE II
OBTAINED RESULTS OF THE IKM METHODOLOGY APPLIED TO THE 3-DOF ROBOTIC FINGER.

$\mathbf{p} = [p_x \quad p_y \quad p_z]^T$ [mm]	ϕ_{init} [Deg]	q_0 [Deg]	q_1 [Deg]	q_2 [Deg]	q_3 [Deg]	ϕ [Deg]	N. iterations	Time [ms]	ε [mm]
$\mathbf{p} = [-8 \quad 0 \quad 106]^T$	97.93°	0	56.84791	62.8957	42.3640	162.1076	113	3.4	0.227
$\mathbf{p} = [-62 \quad 0 \quad 107]^T$	125.40°	0	99.9838	37.8921	25.9202	163.7961	68	2.0	0.344
$\mathbf{p} = [-81.7 \quad 0 \quad 16]^T$	177.85°	0	132.6782	69.9494	46.8452	249.4720	126	3.8	0.111
$\mathbf{p} = [-24.1 \quad 0 \quad 67.4]^T$	118.03°	0	62.3796	90.9328	60.97	212.2912	169	5.1	0.186

for implementation in real-time controllers. Moreover, we can observe in Table 2 the accuracy of the approximation, yielding values for ε considerably small.

It should be mentioned that this model has been implemented in real-time in a PID-type position controller, where a series of points in Cartesian space were proposed and transformed into joint space. The obtained values served as setpoints for the trajectory generation in joint space. The proposed points in Cartesian space are the same as in Table II. Figure 7 shows the obtained positioning of the finger in real-time seen in the finger plane. The magenta dots are the positions to be reached within the workspace, the dotted line is the resulting displacement, and the solid line represents the lateral section of the workspace.

VI. CONCLUSIONS

In this paper, we present a new methodology allowing to solve the IKM problem in underactuated 3R mechanisms with coupling such as robotic fingers. The calculation of IKM in such mechanisms is complex and finding a solution analytically is practically impossible. Our proposal consists in solving iteratively the set of equations that define the kinematics of the mechanism, which are formulated by geometrical analysis, and the FKM of the system. This method is an attractive solution to deal with this problem. The present methodology is applicable in systems such as robotic fingers where the DIP joint is passively coupled to the PIP joint in an attempt to mimic the kinematics of human fingers. The proposed method was used to solve the IKM of a robotic finger intended to be integrated into a future multi-fingered gripper. To validate its performances, four reference coordinates were proposed within the workspace of the finger. The obtained results showed great effectiveness in the estimations. The obtained results also showed that the solutions are found in few iterations, which is suitable for the real-time implementation of the algorithm.

ACKNOWLEDGMENTS

This research was supported by TraceBot project. TraceBot has received funding from the European Union's H2020-EU.2.1.1. INDUSTRIAL LEADERSHIP programme (grant agreement No 101017089).

REFERENCES

[1] C. Melchiorri and M. Kaneko, "Robot hands," in *Springer Handbook of Robotics*. Springer, 2016, pp. 463–480.

[2] B. He, S. Wang, and Y. Liu, "Underactuated robotics: a review," *International Journal of Advanced Robotic Systems*, vol. 16, no. 4, p. 1729881419862164, 2019.

[3] F. Iida, "Biologically inspired motor control for underactuated robots–trends and challenges," *Robot Motion and Control 2009*, pp. 145–154, 2009.

[4] Q. Wang, Q. Quan, Z. Deng, and X. Hou, "An underactuated robotic arm based on differential gears for capturing moving targets: Analysis and design," *Journal of Mechanisms and Robotics*, vol. 8, no. 4, 2016.

[5] B. He, P. Zhang, W. Liu, and W. Tang, "Dynamics analysis and numerical simulation of a novel underactuated robot wrist," *Proceedings of the Institution of Mechanical Engineers, Part B: Journal of Engineering Manufacture*, vol. 231, no. 12, pp. 2145–2158, 2017.

[6] T. H. Koh, M. W. Lau, E. Low, G. Seet, S. Swei, and P. L. Cheng, "A study of the control of an underactuated underwater robotic vehicle," in *IEEE/RSJ International Conference on Intelligent Robots and Systems*, vol. 2. IEEE, 2002, pp. 2049–2054.

[7] R. Cabás, L. M. Cabas, and C. Balaguer, "Optimized design of the underactuated robotic hand," in *Proceedings 2006 IEEE International Conference on Robotics and Automation, 2006. ICRA 2006.* IEEE, 2006, pp. 982–987.

[8] P. Liu, M. N. Huda, L. Sun, and H. Yu, "A survey on underactuated robotic systems: bio-inspiration, trajectory planning and control," *Mechatronics*, vol. 72, p. 102443, 2020.

[9] K. J. Van-Zwieten, K. P. Schmidt, G. J. Bex, P. L. Lippens, and W. Duyvendak, "An analytical expression for the dip–pip flexion interdependence in human fingers," *Acta of Bioengineering and Biomechanics*, vol. 17, no. 1, pp. 129–135, 2015.

[10] M. H. Abdelhafiz, E. G. Spaich, S. Dosen, and L. N. A. Struijk, "Bio-inspired tendon driven mechanism for simultaneous finger joints flexion using a soft hand exoskeleton," in *2019 IEEE 16th International Conference on Rehabilitation Robotics (ICORR)*. IEEE, 2019, pp. 1073–1078.

[11] M. Grebenstein, M. Chalon, M. A. Roa, and C. Borst, "Dlr multi-fingered hands," *Humanoid Robotics: A Reference*, pp. 1–41, 2018.

[12] J. Butterfaß, M. Grebenstein, H. Liu, and G. Hirzinger, "Dlr-hand ii: Next generation of a dextrous robot hand," in *Proceedings 2001 ICRA. IEEE International Conference on Robotics and Automation (Cat. No. 01CH37164)*, vol. 1. IEEE, 2001, pp. 109–114.

[13] J. Martin and M. Grossard, "Design of a fully modular and backdrivable dexterous hand," *The International Journal of Robotics Research*, vol. 33, no. 5, pp. 783–798, 2014.

[14] J. Angeles, *Fundamentals of robotic mechanical systems: theory, methods, and algorithms*. Springer, 2003.

[15] B. Siciliano, L. Sciavicco, L. Villani, and G. Oriolo, *Robotics: Modelling, Planning and Control*. Springer, 2009.

[16] L.-W. Tsai, *Robot analysis: the mechanics of serial and parallel manipulators*. John Wiley & Sons, 1999.

[17] B.-H. Kim, "A method for inverse kinematic solutions of 3r manipulators with coupling," in *International Conference on Intelligent Robotics and Applications*. Springer, 2013, pp. 742–749.

[18] E. L. Secco, A. Visioli, and G. Magenes, "Minimum jerk motion planning for a prosthetic finger," *Journal of Robotic Systems*, vol. 21, no. 7, pp. 361–368, 2004.

[19] J. C. Mason and D. C. Handscomb, *Chebyshev polynomials*. Chapman and Hall/CRC, 2002.

[20] K. M. Lynch and F. C. Park, *Modern robotics*. Cambridge University Press, 2017.

[21] S. Cobos, M. Ferre, M. S. Uran, J. Ortego, and C. Pena, "Efficient human hand kinematics for manipulation tasks," in *2008 IEEE/RSJ International Conference on Intelligent Robots and Systems*. IEEE, 2008, pp. 2246–2251.

[22] J. M. Escorcia-Hernandez, M. Grossard, and F. Gosselin, "Task-oriented methodology combining human manual gestures and robotic grasp stability analyses: application to the specification of dexterous robotic grippers," *Journal of Mechanical Design*, vol. 145, no. 4, 2023.